Available online at www.sciencedirect.com
ScienceDirect
Advances in Space Research 40 (2007) 1126–1139
ADVANCES IN SPACE RESEARCH (a COSPAR publication)
www.elsevier.com/locate/asr

The role of the global electric circuit in solar and internal forcing of clouds and climate

Brian A. Tinsley [a,*], G.B. Burns [b], Limin Zhou [a,c]

[a] University of Texas at Dallas, WT15, Box 830688, Richardson, TX 75083-0688, USA
[b] Australian Antarctic Division, Kingston 7050, Australia
[c] State Key Laboratory of Environmental Geochemistry, Institute of Geochemistry, Chinese Academy of Sciences, Guiyang, China

Received 16 October 2006; received in revised form 1 January 2007; accepted 10 January 2007

Abstract

Reports of a variety of short-term meteorological responses to changes in the global electric circuit associated with a set of disparate inputs are analyzed. The meteorological responses consist of changes in cloud cover, atmospheric temperature, pressure, or dynamics. All of these are found to be responding to changes in a key linking agent, that of the downward current density, J_z, that flows from the ionosphere through the troposphere to the surface (ocean and land). As it flows through layer clouds, J_z generates space charge in conductivity gradients at the upper and lower boundaries, and this electrical charge is capable of affecting the microphysical interactions between droplets and both ice-forming nuclei and condensation nuclei.

Four short-term inputs to the global circuit are due to solar activity and consist of (1) Forbush decreases of the galactic cosmic ray flux; (2) solar energetic particle events; (3) relativistic electron precipitation changes; and (4) polar cap ionospheric convection potential changes. One input that is internal to the global circuit consists of (5) global ionospheric potential changes due to changes in the current output of the highly electrified clouds (mainly deep convective clouds at low latitudes) that act as generators for the circuit.

The observed short-term meteorological responses to these five inputs are of small amplitude but high statistical significance for repeated J_z changes of order 5% for low latitudes increasing to 25–30% at high latitudes. On the timescales of multidecadal solar minima, such as the Maunder minimum, changes in tropospheric dynamics and climate related to J_z are also larger at high latitudes, and correlate with the lower energy component ($\sim$1 GeV) of the cosmic ray flux increasing by as much as a factor of two relative to present values. Also, there are comparable cosmic ray flux changes and climate responses on millennial timescales. The persistence of the longer-term J_z changes for many decades to many centuries would produce an integrated effect on climate that could dominate over short-term weather and climate variations, and explain the observed correlations.

Thus, we propose that mechanisms responding to J_z are a candidate for explanations of sun–weather–climate correlations on multidecadal to millenial timescales, as well as on the day-to-day timescales analyzed here.

Keywords: Global electric circuit; Climate; Cloud microphysics; Cosmic rays

1. Introduction

1.1. Ionosphere-earth current density variations

The current density J_z that flows downwards from the ionosphere to the land or ocean surface shows day-to-day variations associated with solar activity and with internal changes in the global atmospheric electric circuit. The ionosphere is at a potential V_i of about 250 kV, maintained by an upward current of about 1000 A, from the totality of thunderclouds and other highly electrified clouds over the globe (Williams, 2005). The magnitude of the return current J_z is 1–6 pA m^{-2}, distributed over the globe, with the largest variation in average current density a function of geographical location, as has been found in observations and models (Hays and Roble,

* Corresponding author.
E-mail addresses: Tinsley@UTDallas.edu (B.A. Tinsley), Gary.Burns@aad.gov.au (G.B. Burns).

0273-1177/$30
doi:10.1016/j.asr.2007.01.071

1979; Sapkota and Varshneya, 1990; Tinsley and Zhou, 2006). J_z varies in response to changes in external and internal forcing agents. The external agents are (1) the galactic cosmic ray (GCR) flux; (2) solar energetic particles, or SEP (mainly MeV proton) events; (3) relativistic (MeV) electron precipitation from the radiation belts; and (4) horizontal ionospheric potential distributions within the polar caps that are associated with solar wind magnetic field changes, and are superimposed on the otherwise uniform global ionospheric potential. The magnitude of J_z also varies globally, in response to the internal forcing by (5) variations of around $\pm 20\%$ in the 1000 A current output of the highly electrified clouds, that are reflected in global changes in V_i.

Other sources of variability in J_z include regional and global changes in the resistivity of the atmosphere due to changing natural and anthropogenic aerosol loading. There are few reliable measurements of the solar and global variations of J_z, because of instrumental difficulties for extended measurements, with a great deal of local electrical 'meteorological' noise from moving conductivity inhomogeneities on time scales of hours to weeks and spatial scales of tens to hundreds of km at most land stations, even in 'fair' weather. On longer time and greater spatial scales, and higher in the atmosphere these noise variations average out. The technique of superposed analysis is particularly useful in bringing out the effects of day-to-day forcing, as much of the noise is averaged out when several tens of events are averaged.

The experimental validation of the global circuit models has been mainly through much averaging of the near surface electric field E_z measurements, where $E_z = J_z/\sigma$, with σ being the conductivity of the near-surface measurement location. There is much variation of σ due to inhomogeneities in radon, local aerosols, and humidity variations, exacerbated by vertical convection and turbulence. Better global signatures of E_z and J_z have been obtained by averaging data from oceanic, high-mountain, and polar ice cap sites, or from balloons. (Israël, 1973; Reiter, 1992; Bering et al., 1998; Burns et al., 2005; Mühleisen et al., 1971; Hu and Holzworth, 1996), and these are generally consistent with the response of the models, for example to diurnal changes in tropical thunderstorm activity, and to decadal changes in the GCR flux. Changes in J_z as a result of ionospheric potential changes in the polar caps have been modeled by Park (1976) and Tinsley and Heelis (1993), and compared with measured E_z values by Tinsley et al. (1998) and Burns et al. (2006). Indirect evidence for effects on J_z of precipitation of relativistic electrons (from the radiation belts) into the stratosphere, at times of high stratospheric aerosol loading, has been discussed by Tinsley et al. (1994), Kirkland et al. (1996), Kniveton and Tinsley (2004) and Tinsley and Zhou (2006). The effects on the global circuit of SEP precipitation into the polar caps have been measured by Holzworth and Mozer (1979).

1.2. Correlations of weather and climate with solar activity

For many years correlations of various meteorological parameters with solar activity on a wide range of time scales have been published. We focus on the day-to-day and centennial through millennial periods. On the day-to-day timescale there is not the ambiguity that there is on the decadal timescale between solar irradiance effects and space weather (particles and fields) effects as forcing agents for the meteorological changes. As will be reviewed in Section 3, the onset times and durations of the meteorological responses agree with those of the space weather forcing agents. No significant correlations on this timescale are found with either total solar irradiance or the UV irradiance. The different time variations of the sources and the different propagation times to the Earth ensure this. The results will demonstrate that J_z by itself forces cloud and weather changes. On the centennial and millennial timescales the proxies for CGR flux and the associated J_z show larger changes than on the decadal timescale. The persistence of the changes for periods of many decades through centuries means that the integrated effects of the GCR and J_z changes could dominate over shorter-term variations due to aerosol and weather and climate noise.

The observations showing clear correlations on the day-to-day timescale have been published by Schuurmans and Oort (1969), Wilcox et al. (1973), Mansurov et al. (1974), Olson et al. (1975), Larsen and Kelley (1977), Misumi (1983), Tinsley and Deen (1991), Pudovkin and Veretenenko (1995), Kirkland et al. (1996), Todd and Kniveton (2001), Veretenenko and Thejll (2004), Kniveton and Tinsley (2004) and Roldugin and Tinsley (2004). Also new results by Burns et al. (2007) show high latitude surface pressure changes in response to J_z changes, on the day-to-day timescale, that are of the same nature as responses to J_z changes caused by the solar wind; however, in this case they are due to J_z changes resulting from ionospheric potential changes due to variations in the low latitude highly electrified convective cloud generators of the global circuit.

Clear correlations on the centennial through millennial periods are shown by Eddy (1977), Stuiver et al. (1995), Ram and Stolz (1999), Hong et al. (2000), Bond et al. (2001), Neff et al. (2001) and Wang et al. (2005a,b). We will show that both on the day-to-day through millennial timescales such responses to solar activity can be understood in terms of cloud microphysical responses to the J_z changes. Fig. 1 illustrates the flow of J_z through gradients in conductivity at the boundaries of clouds, creating space charge in accordance with Gauss's Law. All of the responses described above are consistent with the hypothesis that the scavenging in clouds of ice-forming and/or condensation nuclei is influenced by this space charge.

1.3. Scavenging processes

There appear to be two main channels for electrical effects on clouds of scavenging processes. One is the

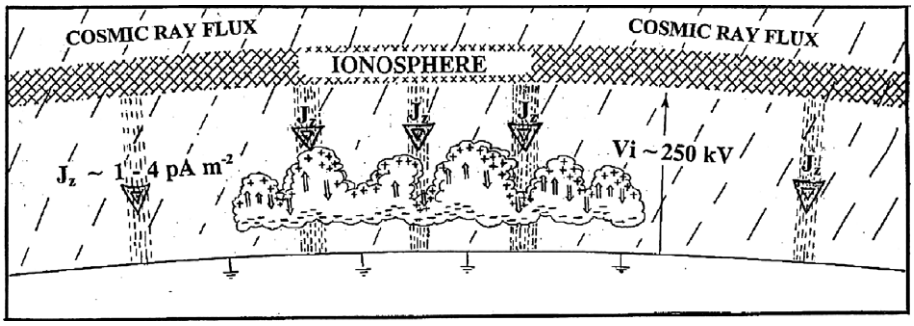

Fig. 1. Schematic of space charge accumulation at the conductivity gradients at the boundaries of layer clouds, due to the flow of ionosphere-earth current density, J_z, through the gradients. The charges attach to aerosol particles and droplets, affecting the cloud microphysics. The columns of J_z represent a continuous flow of current density everywhere throughout the atmosphere.

electrical enhancement of scavenging (electroscavenging) by supercooled droplets (−15 to 0 °C) of aerosol particles that constitute ice-forming nuclei, or IFN (Tinsley et al., 2001). This increases the rate of production of primary ice by contact ice nucleation, leading to greater rates of precipitation by the Bergeron–Findeisen mechanism (Cotton and Anthes, 1989); it would be associated with changes in the latent heat release from deep clouds of winter storms, and may explain observations of changes in storm dynamics and the general circulation (Tinsley and Deen, 1991). For thinner layer clouds, there would be a reduction in cloud lifetime and cloud cover, with the capability of explaining changes in atmospheric circulation through changes in the radiation balance and tropospheric heating.

The other main channel is for an increase in scavenging of the larger cloud condensation nuclei (CCN), along with various other aerosol particles, by the short-range image electrical forces, accompanied by a protection by the long-range repulsive force of the smallest CCN and other small particles from scavenging by other processes, (i.e., from scavenging by Brownian diffusion and phoretic (evaporation) scavenging) as discussed by Tinsley (2004). In this case, the result is an increase in concentration and narrowing of both the CCN and the droplet size distributions in episodes of continuing cloud formation (the Twomey effect) accompanied by a reduction in precipitation and an increase in cloud lifetime. Again, there are plausible consequences for cloud cover, storm dynamics, the atmospheric radiative balance, and tropospheric dynamics.

Variations in the cosmic ray flux from the galaxy that are thought to occur on the million-year timescale (Shaviv, 2002) may be important. Also, changes in the Earth's geomagnetic field on millennial timescales will affect the latitude variation of the GCR flux and thus that of J_z (see Section 6.4).

We now discuss in more detail the global circuit; the observational evidence for forcing by J_z; modeling of space charge production in clouds; models of the electrical effects on cloud microphysics; and implications for climate change in response to long-term changes in J_z. The J_z changes that can potentially affect clouds and climate are due to varying solar activity, varying sources of cosmic ray flux in the galaxy, and varying surface temperatures at low latitudes affecting the output of the thundercloud generators there.

2. The global circuit

Fig. 2 is a schematic diagram of a section of the global circuit in the dawn–dusk magnetic meridian. The ionosphere forms a conducting shell, which is charged by highly electrified clouds, mainly low latitude thunderclouds as represented for equatorial latitudes. The diurnal variations of the global upward current of about 1000 A creates a diurnally varying ionospheric potential V_i that averages about 250 kV, which is essentially an equipotential out to about 50° geomagnetic latitude. At any location away from these generators the downward return current density J_z is 1–6 pA m^{-2}, depending on the resistance R of the column of unit cross section there.

At high magnetic latitudes the potentials generated by the relative velocity between the magnetized solar wind plasma and the Earth generates additional potential distributions superimposed on the global ionospheric potential V_i, as indicated in Fig. 2. The north–south component of the solar wind magnetic field B_z leads to a dawn–dusk potential difference of magnitude 30–150 kV across each polar cap, and the east–west component B_y leads to a potential difference appearing between the northern polar cap ionosphere and the southern polar cap ionosphere, with a magnitude that is typically a few tens of kilovolts, with the sign and magnitude that depend on the sign and magnitude of B_y. The sign of B_y depends on whether the solar wind magnetic field points towards or away from the sun, and this polarity depends on the sector structure of the solar wind (Zhao and Hundhausen, 1983) that rotates with the sun. Usually the sector structure is stable for a few months at a time, so that B_y tends to vary with the sun's 27 day rotation period. When four-sector or six-sector structure replaces the simpler two-sector structure, additional periodicities of 13 days or 9 days, with irregular phasing, can also appear.

The vertical column resistance R at any location is mainly determined by the altitude of the surface and the flux of GCR at that latitude (e.g., Tinsley and Zhou,

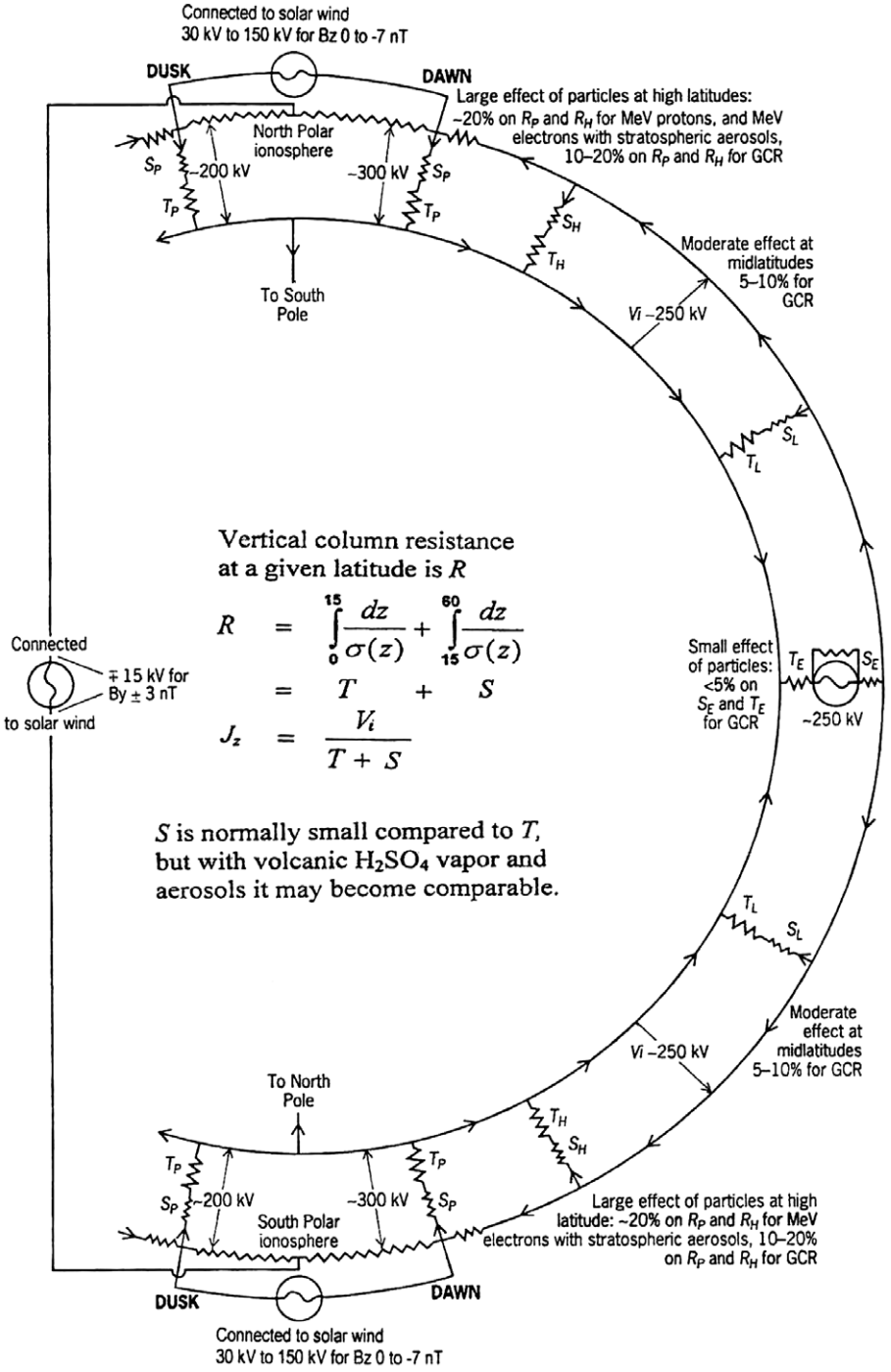

Fig. 2. Schematic of a section through the global atmospheric electric circuit in the dawn–dusk magnetic meridian. The tropospheric and stratospheric column resistances at a given location are represented by T and S, with subscripts referring to equatorial, low, middle, high, and polar latitudes. The geometry is essentially plane-parallel, with only small changes in T due to changes in cosmic ray fluxes at low latitudes, but large changes in T and S due to cosmic ray and other energetic space particle fluxes at high latitudes. The variable solar wind generators affect V_i at high latitudes, and the variable electrified cloud generators affect V_i globally, and volcanic aerosols as well as the energetic particles affect T and S; with all acting together to modulate the ionosphere-earth current density J_z.

2006). This flux creates ion pairs throughout the column, causing it to conduct weakly. There are two additional sources of ion pair production; one is the relativistic electron flux and associated X-ray bremsstrahlung that penetrates down to about 30 km in sub-auroral latitudes (Frahm et al., 1997; Li et al., 2001a,b; Tinsley et al., 1994), and the other is SEP events (Holzworth et al., 1987) that produce stratospheric ionization, excess positive charge, and occasionally a small amount of tropospheric ionization in the polar cap regions. In Fig. 2 the stratospheric and tropospheric contributions to the column resistance at any location are labeled S and T. Then J_z at that

location is given by Ohm's Law: $J_z = V_i/(T + S)$. So any input that modulates V_i or T or S will also modulate J_z.

Fig. 3 is based on the model by Tinsley and Zhou (2006), and shows column resistances R along two meridional sections, at longitudes 92.5° (East Asian) and −72.5° (the Americas). For each longitude the curves for solar maximum and minimum are shown for situations with and without the estimated stratospheric ultrafine volcanic aerosol layer. The layer is located poleward of ±40° geographic latitudes, where the layer column resistance becomes the dominant part of S, and is calculated for the absence of the ionization due to precipitating relativistic electron flux. This ionization is considered to be present most of the time, and to make the ultrafine layer then a good conductor so that S is negligible with respect to T. It is only for periods of a few days when the slow solar wind at the heliospheric current sheet crosses the earth that the precipitating relativistic electron flux falls by an order of magnitude, and R increases and J_z decreases at higher latitudes, during a few years following large explosive volcanic eruptions.

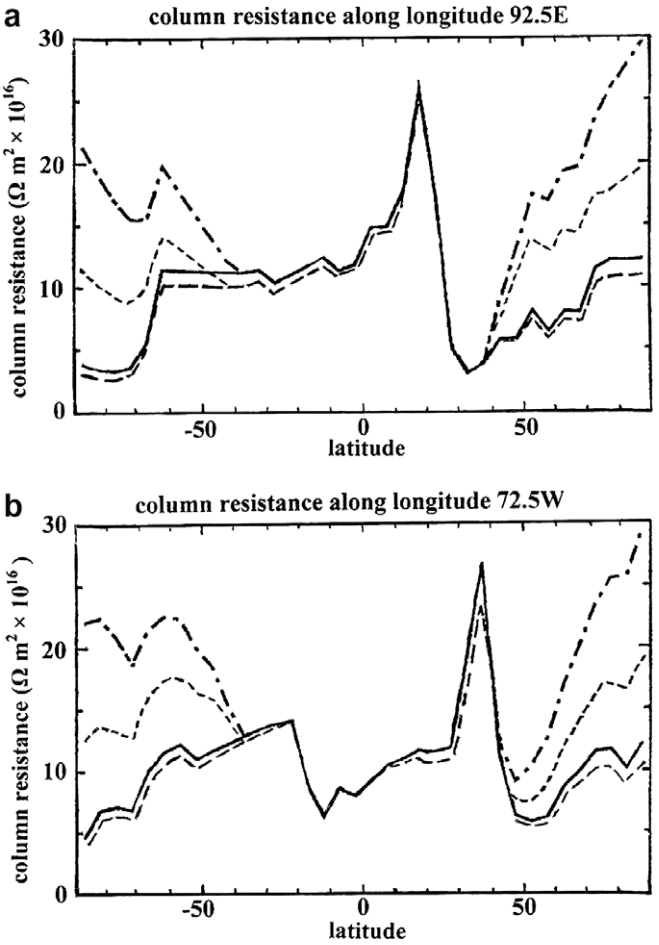

Fig. 3. Profiles of column resistance R along (a) longitude 92.5°E and (b) 72.5°W. The curves are for December conditions, with no stratospheric ion production by relativistic electrons. The solid curves are for solar maximum (cosmic ray minimum) and the large dashed curves for solar minimum, both in the absence of stratospheric ultrafine aerosols. The dot-dashed curves are for solar maximum and the small dashed curves for solar minimum, in the presence of stratospheric ultrafine aerosols. For details see Tinsley and Zhou (2006).

In Fig. 3 the solar cycle variation of cosmic ray flux and conductivity is only a few percent near the magnetic equator, which is near 12°S latitude at −72.5° longitude, and near 12°N latitude at 92.5° longitude. The peaks in column conductivity are due to polluted industrial regions near sea level altitude in each case, and the minima in column conductivity are for the clean high altitude Antarctic plateau and Himalayan regions.

3. Summary of observational evidence

The most unambiguous evidence supporting the concept of variations of atmospheric dynamics driven by J_z changes and consequent cloud changes comes from analysis of the studies, on the day-to-day timescale, that are referenced in Section 1. These can be grouped into categories by the type of external or internal driver. Most categories have been observed in several different epochs as well as in more than one parameter of meteorological response. The meteorological parameters that respond are capable of being influenced by changes in clouds. The responses agree in onset time, and duration with the measured or inferred changes in J_z. The amplitudes of the changes are comparable to the general noise level for these parameters; however the effects emerge with moderate to high statistical significance when some tens of events are analyzed, e.g., by superposed epoch analyses.

None of the studies taken individually make an unambiguous case for a solar/atmospheric electrical/cloud/atmospheric dynamics connection, but it is the purpose of this paper to show, that taken together, in the context of modeled cloud microphysical effects, that they do make a strong case for such a connection.

Fig. 4 is a flow chart summarizing the five categories of short-term influences on J_z and the associated meteorological responses. The labels A to E refer to the five chains of processes, which have in common a J_z change, which links the driver with the meteorological response. They all tend to have strongest effects at higher latitudes. We now provide information on each of these chains.

Effects of short-term GCR flux changes (Forbush decreases, Chain E) have been observed as changes in atmospheric vorticity in winter storms (Macdonald and Roberts, 1960; Tinsley and Deen, 1991) and as changes in high altitude cloud cover (Pudovkin and Veretenenko, 1995; Todd and Kniveton, 2001). Effects of SEP events (Chain D) have been observed as latitudinal gradients in pressure after large solar flares (these are usually accompanied by SEP events) by Schuurmans and Oort (1969) and as changes in atmospheric vorticity (Veretenenko and Thejll, 2004, 2005). The onset times for the responses are less than a day following the onset of the Forbush decrease or SEP event. The vorticity changes associated with SEP events are of opposite sign to those associated with Forbush decreases, consistent with the J_z increases for SEP events

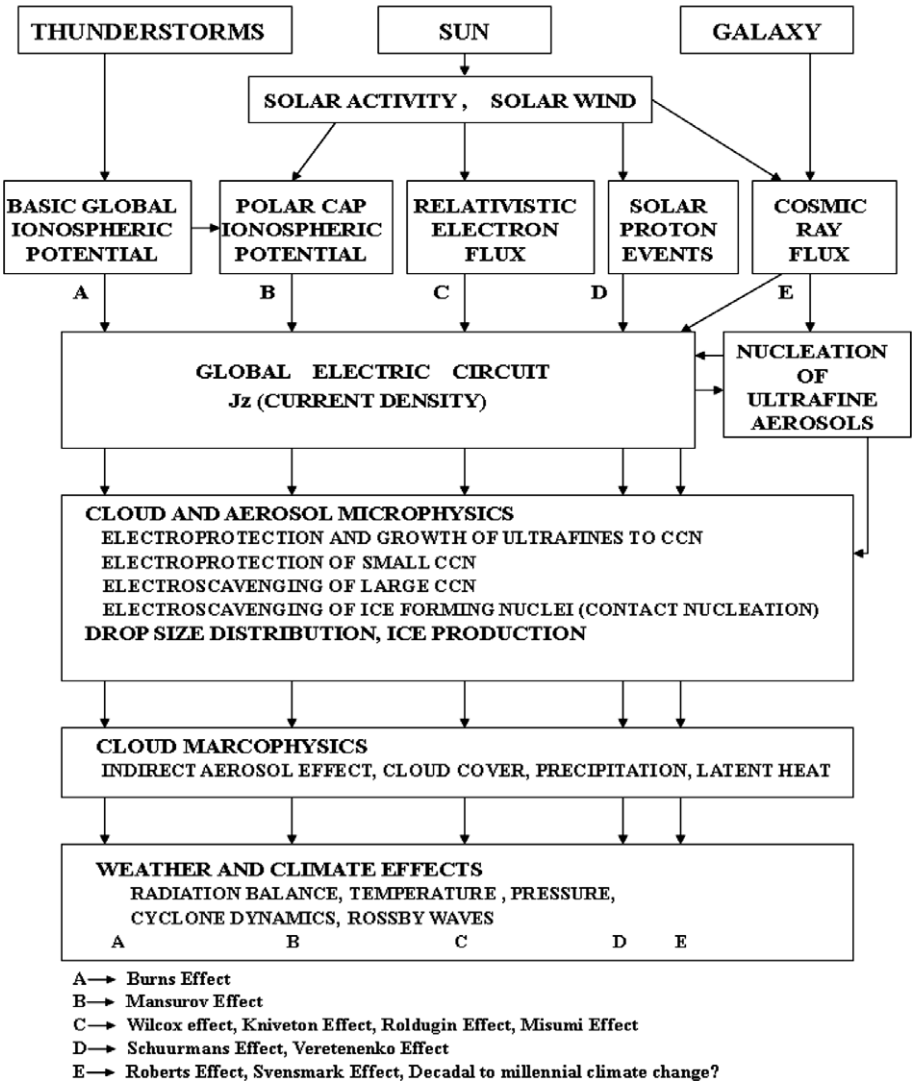

Fig. 4. Processes connecting thunderstorms, solar activity and galactic cosmic ray flux with the global atmospheric electric circuit, cloud and aerosol microphysics, and weather and climate. The five independent forcing agents (A through E) all affect the ionosphere-earth current density J_z, and correlate with meteorological responses via hypothesized chains of cloud microphysical and macroscopic processes as shown. These are named at the bottom of the flowchart, and detailed in the text.

(Holzworth and Mozer, 1979; Holzworth et al., 1987) being opposite to the J_z decreases associated with Forbush decreases (Märcz, 1997; Sapkota and Varshneya, 1990). A combined effect, presumed to be due to SEP events (associated with observed solar flares) followed by Forbush decreases, consisted of vorticity increases followed by decreases (Olson et al., 1975).

Effects of changes in relativistic electron precipitation, for which solar wind magnetic sector boundaries have been used as a marker (Chain C) have been observed in terms of changes in atmospheric vorticity (Wilcox et al., 1973; Larsen and Kelley, 1977; Tinsley et al., 1994; Kirkland et al., 1996); in changes in 500 hPa temperature (Misumi, 1983); in changes in cloud cover (Kniveton and Tinsley, 2004); and in changes in atmospheric transparency (Roldugin and Tinsley, 2004). These effects are clear at times when the stratospheric column resistance S appears to be comparable to the tropospheric column resistance T, e.g., when the stratosphere contains a high concentration of ultrafine aerosol particles following large volcanic eruptions, as modeled by Tinsley and Zhou (2006).

Effects of changes in polar cap ionospheric potential (Chain B, due to solar wind B_y changes as in Fig. 2) were observed in terms of changes in high latitude surface pressure by Mansurov et al. (1974) and Page (1989), (see Tinsley and Heelis, 1993) and with high statistical significance in recent work by Burns et al. (2007). The observed pressure changes were opposite in the Arctic as compared to the Antarctic, consistent with the opposite J_z changes (defined in each polar cap as towards the Earth's surface). For the Burns et al. (2007) observations the range of pressure changes was about 2 hPa, and using the ratio of 0.33 (hPa)/(nT) for the smoothed data (their Table 1) this corresponds to about a 6 nT B_y range. Then, using the ratio

of 2.87 (kV)/(nT) (their Fig. 3) for the associated change in V_i from their use of the Weimer model, this corresponds to a 17 kV change in V_i. Then, using the average ratio of 0.90 (V m^{-1})/(kV) surface electric field change to V_i change (Burns et al., 2006, Fig. 4), we obtain a 15.7 V m^{-1} change in inferred electric field at the surface, with a ratio $\Delta p/\Delta E_z = 2.0/15.7 = 0.13$ (hPa)/(V m^{-1}). The periodicity in these externally forced changes was predominantly the 27-day period of the solar rotation and the solar wind magnetic sector structure.

There is internal forcing of J_z due to the day-to-day changes in ionospheric potential that are due to the day-to-day changes in highly electrified deep convective clouds, mainly in the humid low latitude land areas in Africa, the Americas, and northern Australia/Indonesia. As the temperature and moisture content of the air masses in these regions vary, so does the incidence of large mesoscale convective systems, which produce the highly electrified clouds. These thunderclouds are the main source of the charging current I_t into the ionosphere, that is reflected in the ionospheric potential V_i. (The value of V_i is given by $V_i = I_t R_t$ where R_t is the global total resistance of the return ionosphere-to-earth path, consisting of the sum as resistors in parallel of all the column resistances over the globe. There is also a well-known diurnal variation in V_i due to diurnal heating cycles). The day to day changes in V_i and consequently in J_z can be characterized by a standard deviation from the mean of order 10% (Adlerman and Williams, 1996; Burns et al., 2005, 2006) which is several times larger than the V_i changes due to the solar wind B_y changes. Consequently, a several-times-larger pressure response to this internal forcing, as compared to the B_y forcing, is to be expected. This response has been found in an analysis of Vostok (79°S, 107°E) electric field and pressure data (Burns et al., 2007) shown as Chain A in Fig. 4. The correlation was made with measured near-surface electric field (E_z) changes, which are a proxy for J_z changes. The range of pressure response (Δp) was up to 7 hPa, and the ratio of the observed pressure change, for smoothed data, to the electric field (ΔE_z) change gave a $\Delta p/\Delta E_z$ value of 0.11 (hPa)/(V m^{-1}) (Burns et al., 2007, Table 1). In view of the measurement uncertainties this is essentially the same ratio as was found for the Mansurov effect 0.13 (hPa)/(V m^{-1}).

The responses were found separately for data for 2000 and 2001, and the results for both years are consistent in that the maximum correlation of Δp with ΔE_z occurred with a lag of Δp with respect to ΔE_z of 2–3 days. This same lag of 2–3 days is found in the Vostok pressure response to the external B_y forcing. The agreement of the lags, together with the larger pressure response to the larger internally caused ΔE_z changes, but with essentially the same $\Delta p/\Delta E_z$ ratio as for the externally caused ones, rules out the possibility that ΔE_z and Δp are somehow both separately responding to local meteorological changes.

This example (of the response of a meteorological parameter to a J_z change generated remotely in the atmosphere) is fully consistent with the characteristics of the external electrical forcing. As the use of a hypothesized mechanism to explain a different phenomenon to that for which it was originally proposed, its success in the explanation strongly supports the hypothesis of J_z effects on clouds.

As an explanation for these observations, the mechanism of ion-mediated nucleation (Yu and Turco, 2001) cannot be responsible for chains A through D, because there is no change in ion production in the troposphere. (For reviews of cloud and aerosol microphysics discussing both ion-mediated nucleation and electroscavenging processes as explanations for changes in clouds correlated with changes in GCR flux, see Carslaw et al. (2002) and Harrison and Carslaw (2003)).

4. Space charge production in clouds

The downward current density J_z flows through gradients in conductivity at the boundaries of clouds and aerosol layers creating gradients in electrical field, and space charge density in accordance with Gauss's Law. This charge attaches to droplets and aerosol particles, including CCN and IFN. The amount of such charge on droplets and particles has been modeled by Zhou and Tinsley (in press). Fig. 5 is the result of one model run, showing steps in the calculation of droplet mean charge (p, in Fig. 5(f)) for three different J_z values. The droplets are highly effective in reducing the ion concentration, with the diffusing ions becoming attached to them, and consequently the conductivity is reduced by a factor of between 3 and 30 (Griffiths et al., 1974). The electric field is proportional to the current density and inversely proportional to the conductivity. The magnitude of the space charge, droplet charge, and CCN and IFN charges depends on the gradient of the electric field, and thus it also depends inversely on the thickness of the transition layer from cloudy to clear air. In the runs of Fig. 5 the thickness is 10 m. The uniform central region is representative of any thickness of a central region of a layer cloud. The space charge accumulates as multiple charges on the droplets and on the larger aerosol particles proportional to their radii, with a small fraction remaining in the form of ions. The calculation of the equilibrium ion concentration and aerosol and droplet charges was made following the theory of Hoppel and Frick (1986).

The modeled results for the droplet charges p are consistent with the aircraft measurements over Lake Michigan of Beard et al. (2004) who found charges of about 80 e near cloud tops on droplets of radii about 8 μm, and charges of about −70 e near cloud base on droplet radii of about 6 μm, where e is the elementary charge. The differing signs of the charges at the two boundaries are consistent with the flow of J_z through the cloud, and the magnitudes are sufficient to affect scavenging rates (Tinsley et al., 2001, 2006). The charges on IFN and CCN depend on their radii, and information is needed on the concentrations and size distributions of these in order to calculate scavenging rates.

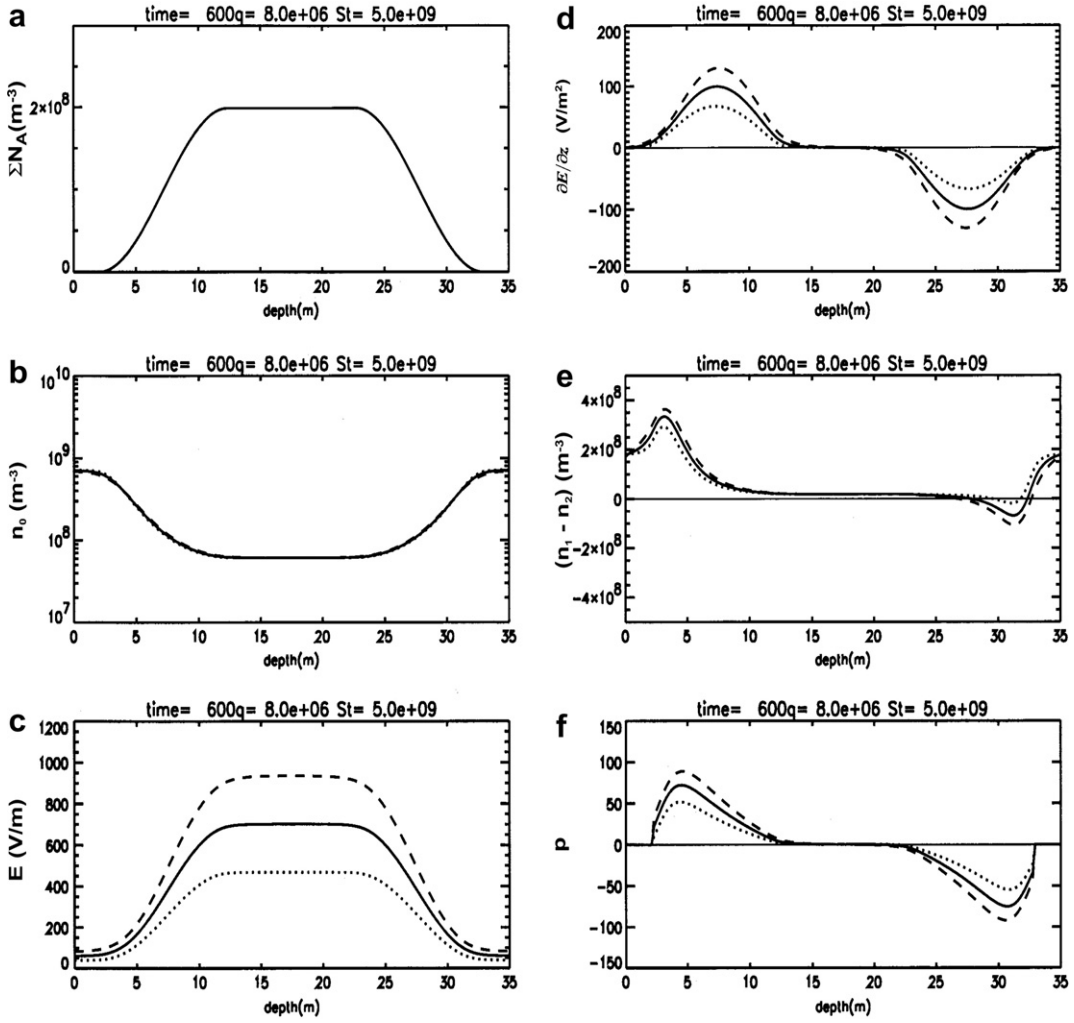

Fig. 5. Results from a model of the production of space charge in clouds (Zhou and Tinsley, in press) as a function of depth in the cloud, in the presence of aerosols and with three values of current density J_z. The dashed lines are for J_z of 4×10^{-12} A m^{-2}; the solid lines for 2×10^{-12} A m^{-2}, and the dotted lines for 1×10^{-12} A m^{-2}. The panels are (a) droplet concentration; (b) ion concentration; (c) electric field; (d) gradient in electric field; (e) difference between positive and negative ion concentration; (f) mean droplet charge, in units of elementary charge. The thin solid lines are zero references.

Also, the charges reported on droplets near cloud tops were in regions of downdrafts, and on those near cloud base in regions of updrafts, so dynamical effects may be important for reducing the widths of the transition layers. In the atmosphere stacked layers of cloud exist, and waves or turbulence within clouds, and these produce alternating gradients of droplet concentration, conductivity, and positive and negative droplet and aerosol charges. Mixing of these oppositely charged droplets and particles could greatly increase the electroscavenging rates (Tinsley et al., 2001).

5. Space charge effects on cloud microphysics

The charges on the droplets and the aerosol particles, including the IFN and the CCN, have an effect on the scavenging rates of the particles by droplets that is a complicated function of droplet size, particle size, particle density and amounts of charge on each. Since there is a long-range Coulomb-type force that is repulsive for objects having charges of the same sign (and attractive for opposite sign) and a short-range image force that is always attractive, trajectory calculations show electrically induced decreases as well as increases in particle scavenging rates (and in particle–particle and droplet–droplet coagulation rates). Fig. 6 shows collision efficiencies, from Tinsley et al. (2006), for aerosol particles with droplets having the same sign charge. The droplets have radii 4, 6 and 10 μm, and the aerosol particles have a density twice that of water, and radii ranging from 0.1 μm up to the radius where the particles are no longer collected (1/2 to 3/4 of the droplet radius for this density). The droplet charge was 100 e in each case, and the particles had charges of 1–100 e, as denoted on the curves. The dashed curve is the collection efficiency for Brownian scavenging. With a relative humidity of 98% there was phoretic scavenging represented by the curve labeled 0 e, which is the asymptote for the family of curves as the charge is reduced to zero.

It can be seen that for the 10 μm radius droplet the effect of increasing particle charge is to increase the scavenging rates for all particles above 0.1 μm radius. (For particle radii

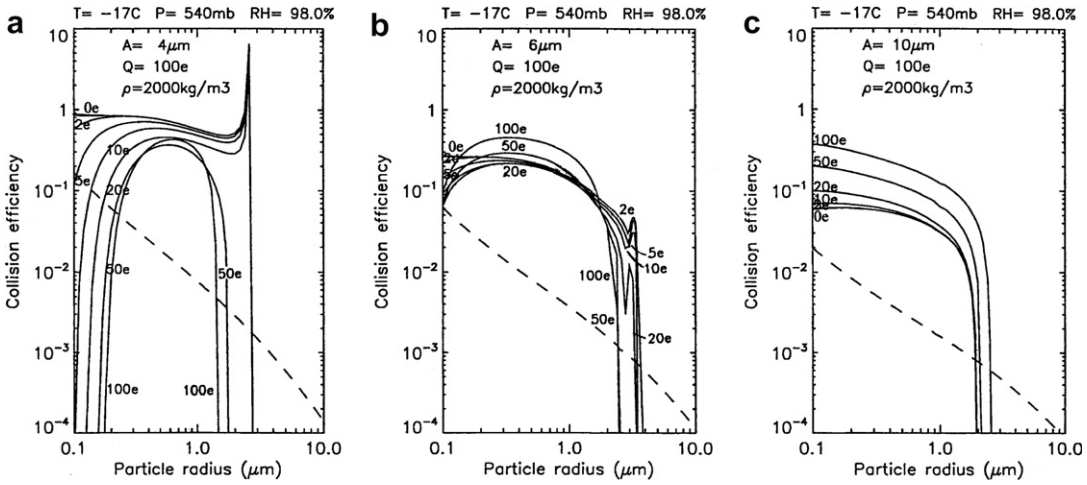

Fig. 6. Effect of electric charges and particle and droplet radii on particle-droplet collision efficiency. The droplet charges are 100 e, the particle density is twice that of water, and the particle charges range from 0 to 100 e as labeled. The temperature and pressure were −17 °C and 540 hPa. The relative humidity was 98% and provided the baseline (curve 0 e) from which electrical effects on scavenging deviated. The collision efficiencies are for droplet of radii (a) 4 μm, (b) 6 μm, and (c) 10 μm.

below 0.1 μm see Tinsley et al. (2001), and for other particle densities see Tinsley et al. (2006).) For the 4 μm droplets the effect of increasing particle charge is to reduce the collision efficiency below the phoretic value at all radii. For particles below 0.7 μm the effect is due to the higher mobility of the smaller particles, allowing the long-range repulsive force to move them away against the airflow, so that it cannot bring them close enough to be into the range of the attractive image force. For particles above 0.7 μm it is the longer time spent near the droplet as the particle fall speed more nearly matches the droplet fall speed that allows the repulsion to take effect. For the 6 μm droplets there is a more complex variation due to the combination of both effects.

Thus the electrical effects on scavenging are likely to be an increase in scavenging rates for the larger particles being scavenged by the larger droplets, with a decrease below the scavenging rates for the smaller particles in the presence of smaller droplets.

For cold (<0 °C) clouds there may be an enhancement of contact ice nucleation with J_z due to increased scavenging of IFN that involves the larger droplets and the larger aerosol particles (Tinsley et al., 2001). So one type of cloud response, applicable to relatively thick winter storm clouds, is an increase in the primary nucleation of ice and in the overall production of ice and precipitation. For stratus type cloud layers the same process would produce a reduction in cloud cover. The above effects on IFN may be invoked as an explanation for observed reductions in winter storm vorticity that correlate with reductions in J_z that are due both to Forbush decreases of GCR (Chain E in Fig. 4) and reductions in relativistic electron flux (Chain C in Fig. 4). This is supported by the observation of the opposite case of increases in winter storm vorticity with increases in J_z due to SEP events (Chain D in Fig. 4) analyzed by Veretenenko and Thejll (2004).

The IFN process could increase the precipitation in winter cyclones, which could conceivably cause a redistribution of the latent heat in the cyclones that increases their ability to extract vorticity from the winter baroclinic pressure gradient. Models of the effect of latent heat redistribution on winter cyclone dynamics are consistent with this scenario (van Delden, 1989; Mallett et al., 1999). The cumulative effects of changes in cyclone strength and increased blocking by them could result in changes in circulation at high latitudes, such as are inferred to have occurred during the late Maunder minimum of solar activity (Luterbacher et al., 2001).

Irrespective of cloud temperature, with increasing J_z and space charge in clouds there is an increase in the scavenging of the larger CCN. However, for the smallest CCN there can be a decrease in scavenging rates below the Brownian and phoretic values, as noted above. A similar effect is likely to be the preservation from scavenging of the ultrafine aerosol particles produced by ion-mediated nucleation, while they are growing to be large enough to act as CCN. This growth is likely in the vicinity of evaporating clouds, where there is a supply of volatiles from evaporating droplets, and where space charge will be present also (Tinsley and Yu, 2004). Thus an increase in J_z may produce, by the above process, a narrowing of the CCN size distribution and an increase in the concentration of the smallest CCN, which become activated into cloud droplets with further cloud formation. These clouds exhibit a larger concentration of smaller average sized droplets, an effect first described by Twomey (1977) that increases cloud lifetime and cloud cover and reduces precipitation. So this is a second type of cloud response to J_z, which can be the opposite of the first in terms of cloud cover change. It provides a possible explanation of observations of changes in cloud cover (Pudovkin and Veretenenko, 1995; Todd and Kniveton, 2001; Kniveton and Tinsley, 2004), and also of changes in atmospheric transparency (Roldugin and Tinsley, 2004) that correlate with inferred J_z changes. In the Kniveton and Tinsley data, with a reduction of J_z of order

10% (Tinsley et al., 1994; Tinsley and Zhou, 2006) a reduction in cloud cover of order 1% was observed.

Two more data sets that fit this type of response are Chains A and B of Fig. 4. As noted earlier, there are surface pressure changes correlated with V_i and J_z changes in the polar caps. This effect is independent of season and volcanic activity, and for chain B is opposite in the Arctic as compared to the Antarctic, consistent with the opposite V_i and J_z changes in the two locations for a given solar wind B_y change. The Mansurov effect (Chain B) has a relatively small amplitude, about 2 hPa maximum excursion, with the mainly 27-day periodicity of the solar wind sector structure. The larger amplitude (Chain A) of surface pressure changes (about 7 hPa maximum excursion) to the larger amplitude J_z changes result from the V_i changes produced by the day-to-day variability of the low latitude thundercloud generators. For both chains there is about a 1 hPa change for each 20 V m^{-1}, corresponding to each 8% change in E_z and J_z. The lag of 2–3 days in the pressure change relative to the changes in V_i and J_z in both responses suggests that a change in cloud cover is acting on the radiative balance of the lower atmosphere, particularly in the trapping of longwave radiation. Then the time constant applies to the accumulating local heating (or cooling) moving air vertically, and out of (or into) the polar cap, and for Coriolis forces to establish a circulation around the polar caps, superimposed in whatever polar vortex already exists.

The involvement of thin, high altitude clouds at these latitudes would seem to preclude a latent heat effect. High clouds were identified by Todd and Kniveton (2001) in the Antarctic cloud responses to Forbush decreases, and in the Kniveton and Tinsley (2004) responses to relativistic electron precipitation. In the Vostok observations also high clouds are required since low clouds are excluded for this effect because atmospheric electricity observations require relatively clear weather. The increase in pressure with increasing J_z implies an increase in atmospheric temperature that implies an increase in the cloud cover at these latitudes. This is consistent in sign with the cloud cover decreases associated with the J_z decreases in the Kniveton and Tinsley (2004) and Roldugin and Tinsley (2004) results. The latter were in nearly clear skies during ozonosonde measurements, implying clouds that were thin or subvisible. The high cloud cover responses to J_z changes caused by relativistic electron precipitation in Chain C (Kniveton and Tinsley, 2004) consisted of opposite changes in zonal means for high latitudes as compared to low latitudes, which is consistent with modeled J_z changes for the simple situation of constant tropospheric current output and no changes in tropospheric conductivity or in ion production.

When the J_z changes are caused by GCR variations, then additional effects of ion concentration changes on space charge, which can be opposite to J_z effects, and on the production of ultrafines by ion-induced nucleation, should be taken into account, and also the poorly known changes in the tropospheric generator output affecting V_i. Changes in J_z will have the same percentage variation at all altitudes, whereas changes in ion production and its effect on space charge, as well as on production of ultrafines, have greater percentage changes at high altitudes. With opposing effects of J_z as compared to ion production there may be opposite effects on cloud lifetime and cloud cover at high altitudes as compared to low altitudes. Further complexity is to be expected on regional scales due to the different responses of cold and warm clouds, and to differences in CCN and IFN concentrations in maritime as opposed to continental clouds.

In view of the complex dependence of the electroscavenging effects on droplet and particle size, detailed dynamical models of clouds, which include time dependency and taking into account different temperature and aerosol environments, are needed to adequately model the regional effects on clouds of the GCR flux and J_z and their changes. Thus, it is not surprising that clear patterns of cloud correlations when both GCR and J_z changes occur emerge only when zonal averages are made for particular altitudes, as in Usoskin et al. (2004). To interpret the complex responses found by Pallé et al. (2004), Pallé (2005) and Voiculescu et al. (2006) will require much more detailed models of cloud response to J_z and ionization changes than are presently available.

This discussion of electrical effects on aerosol and cloud physics is not meant to be definitive or exclusive – rather, its purpose is to stimulate research to examine chains of processes that can be quantitatively modeled to compare with the observations of meteorological responses to J_z and GCR changes.

6. Implications for decadal through Milankovitch-timescale climate change

6.1. Importance of GCR and V_i changes

In the absence of stratospheric volcanic ultrafine aerosols that sensitize the global circuit to relativistic electron precipitation, the main drivers of J_z and cloud responses would be variability in the GCR flux, for which the J_z change is strongly latitude dependent, and variations in V_i due to changes in the electrified cloud generators, which produce J_z changes independent of latitude. Also, V_i changes could be due to GCR changes affecting the generators, or to changes in atmospheric temperature at the location of the generator. While the effects of SEP events and changes in polar cap ionospheric potential are valuable for use in diagnosing the mechanism, they are short lived, or average out in the course of a year, so have little effect on climate timescales.

6.2. Ambiguity with irradiance mechanisms

On the timescale of the solar cycle (9–13 years) there are variations in total solar irradiance (of order of magnitude

0.1%); solar UV irradiance (~1%); and GCR flux (~10% as an average over latitude). There are numerous reports of correlations of climate parameters with the solar cycle (Herman and Goldberg, 1978; Hoyt and Schatten, 1997; Haigh, 1996; Shindell et al., 1999; Tinsley and Yu, 2004) mostly attributing the correlations to irradiance variations, but there is ambiguity as to whether the mechanism is actually due to irradiance variations, rather than electrical effects on clouds.

The largest GCR flux changes are at high latitudes. On the solar cycle timescale neutron monitor data show that they are about a factor 3–5 larger than at low latitudes. So on longer timescales the J_z and cloud changes would be similarly larger at high latitudes, with J_z increasing for increasing GCR flux.

On the timescale of multidecadal minima of solar activity, such as the Spörer minimum (1410–1590 AD), the Maunder minimum (1645–1715) and the Dalton minimum (1795–1825) large increases in the high latitude fluxes of GCR as represented by ^{10}Be and ^{14}C concentrations have been reported in polar ice and other natural archives. For the Maunder minimum, the flux of lower energy GCR in polar regions that produces ^{10}Be increased by about 100% relative to present values (McCracken et al., 2004). This is several times larger than the solar cycle variation. During such extended minima, and for corresponding ^{14}C changes on millennial timescales, there are strong correlations with data on climate change at mid to high latitudes, such as in historical records or proxies such as Δ^{18}O (Eddy, 1977; Stuiver et al., 1995; Ram and Stolz, 1999; Hong et al. (2000); Bond et al., 2001; Neff et al., 2001; Wang et al., 2005a,b).

In contrast to the increases of the GCR flux on the millennial and multidecadal timescale that are several times larger than the solar cycle variability, there seems little reason to expect irradiance changes that could be larger than their solar cycle variations. As has been pointed out by Foukal (2003) and Foukal et al. (2004), the irradiance changes needed in models to explain such climate variations had included a long-term change of irradiance by 0.24% (Lean et al., 1995) that was thought to have been justified by measurements of stellar variability, but these are now suspect. Theoretical models of solar thermodynamics are discouraging in this context also. The analysis of Stott et al. (2003) showed that the global temperature change over the 20th century that correlated with solar activity was about twice that which would have been caused by this no-longer-justified long-term change. Without the long-term change, the discrepancy between irradiance-driven models and atmospheric temperature changes is greater, and during the Maunder minimum it is close to an order of magnitude. Consistent with this, as pointed out by Lean et al. (2002), and especially by Wang et al. (2005b) the theory of changes in open and closed solar magnetic flux suggests that during the Maunder minimum (in comparison with contemporary solar minima) the decreases in irradiance would not have been more than about a third of the solar maximum-to-minimum decrease.

Consequently, the increased amplitude of GCR and J_z changes for the multidecadal solar minima, compared to solar cycle changes, in conjunction with the absence of observational or theoretical justification for significant reductions in irradiance, compared to the solar cycle changes, strengthens the arguments for GCR and J_z changes being a strong component of solar activity-caused climate change on the multidecadal through millennial timescales. Thus we suggest that, instead of regarding the GCR flux changes as merely a proxy for irradiance changes, the GCR and J_z changes should be considered as independent climate forcing agents.

6.3. Uncertainty of V_i response to GCR change

At low latitudes it is not clear whether J_z would increase or decrease with increasing GCR flux, because it is not clear how the current output of the electrified cloud generators responds to GCR changes. As discussed by Tinsley and Zhou (2006), if the current output remains constant with increasing GCR flux, then J_z will decrease a small amount at low latitudes while it increases a larger amount over a smaller area at high latitudes. However, if the generator output increases by more than about 7% with the (latitude dependent) increase in GCR flux from solar maximum to solar minimum, then J_z will increase at all latitudes.

Although atmospheric electricity measurements have been made for more than a century, the nature of the V_i change with GCR flux change (using inverted sunspot number as a proxy) remains uncertain (Israël, 1973; Olson, 1983; Meyerott et al., 1983; Tinsley, 1996). The data are noisy and sparse, and if a pattern can be discerned, it seems to have been for V_i maxima at solar maxima, up to about 1963, when there was a large perturbation due to the large explosive eruption of the Agung volcano. Atmospheric nuclear tests in the late 1950s and early 1960s were also a perturbing factor. From the late 1960s on the balloon measurements for V_i shown by Meyerott et al. (1983, their Fig. 4) suggest a 15–20% increase in V_i from sunspot maximum to a maximum at solar minimum, i.e., V_i increasing with increasing GCR flux. This is also the case for the aircraft and balloon data presented by Markson (1983, his Fig. 6). The balloon measurements of J_z by Olson (1983, his Fig. 2) over Lake Superior show about a 40% increase in J_z from solar maximum to solar minimum. The solar cycle variation of column resistance above Lake Superior from the model of Tinsley and Zhou (2006) was about 10%. Thus the smaller modeled J_z variation than observed suggests that there was an increase of V_i from solar maximum to solar minimum of tens of percent.

Factors that were different before the 1960s as compared to afterwards were the very low stratospheric sulfate aerosol loading (due to the absence since the early 20th century of large explosive volcanic eruptions); the lower level of anthropogenic sulfate aerosols in the atmosphere, and the generally lower level of solar activity. It is not clear from

theory what the net effect of these on the output of current from highly electrified clouds would be.

Since we expect cloud cover to respond to J_z variations on the quasi-decadal and longer timescales in the same way as for the day-to-day J_z changes reviewed earlier, it is possible that the low altitude cloud variations of a few percent correlated with the GCR flux (Svensmark and Friis-Christensen, 1997) are also due to J_z variations, that for low latitudes as well as high increase with increasing GCR flux. Nevertheless, there are many non-J_z factors that produce interannual variability in cloud cover, and many non-GCR inputs that affect V_i, so the above reasoning must remain speculative. What is needed is a well calibrated suite of atmospheric electricity observations from several clean high altitude sites, maintained over several decades.

6.4. Effects of geomagnetic field changes

Reductions in the geomagnetic dipole moment decrease the latitudes at which low energy GCR particles can enter the atmosphere, resulting in greater ionization at lower latitudes. Because the cutoff for the lower energy GCR particles is about 60° geomagnetic latitude at present, above these latitudes there would be no change in the incoming flux with dipole moment reductions. The GCR flux at middle and low latitudes would increase, but as discussed earlier, it is not clear how V_i would change, if at all. There could be increases in J_z, at mid-latitudes and decreases at high and low latitudes. Thus, no dramatic climate change would necessarily have occurred for the dipole moment reduction to about 10% of its present value during the Laschamp event 40,000 years ago (Muscheler et al., 2004).

6.5. Milankovitch time scales

A widely recognized driver for climate change on Milankovitch time scales is the change in seasonal insolation at high northern latitudes due to orbital changes. These result in tropical land temperatures cooler by as much as 5 °C during ice ages (Ruddiman, 2001, p. 298), and these may lead to a large reduction of deep convection and thunderstorm activity, and corresponding reductions in J_z globally. According to the summary by Williams (2005) a 1 °C increase in temperature generates about a 50% increase in lightning on a diurnal to semiannual timescale, and about a 20% increase on annual to decadal timescales. Consequent changes in cloud cover could act as a latitude-dependent feedback process; dependent on whether, at a given latitude, contact ice nucleation or CCN scavenging was predominant. This process would extend, with the same sign, into both hemispheres. This is in contrast to the seasonal insolation changes at high latitudes in the two hemispheres, due to precession, that are of opposite sign.

An independent driver for climate change on Milankovitch time scales is in terms of a change in electrified cloud output directly due to orbital changes. At present the low latitude insolation is about 7% greater at perihelion (January) as compared to aphelion (July). Precession moves this maximum through the seasons with about a 23,000 year period. At present the observed maximum in thundercloud activity is found in the northern summer, with the July values greater than the January value by about 10% (Adlerman and Williams, 1996; Burns et al., 2005). This maximum is attributed to the amount of low latitude land suitable for generating thunderstorms being greater in the northern hemisphere than in the southern hemisphere, so that the maximum thundercloud output is found in the northern summer, in spite of the 7% weaker irradiance then. In 11,500 years when perihelion is at the time of the northern hemisphere summer, the July/January ratio could be several times larger, reflecting a 23,000 year periodicity in V_i, J_z and cloud cover.

Furthermore, the 41,000 year Milankovich period, which is due to changes in obliquity of the Earth's axis, would also be present independently in the output of the thunderstorm generators. This is because of the same preponderance of northern hemisphere thunderstorm-generating land masses. With a more nearly overhead sun for the northern summer maximum in thunderstorm output, the 41,000 year periodicity would also be generated in V_i, J_z and cloud cover as the obliquity changed.

7. Conclusions

Meteorological effects in the form of cloud cover changes, atmospheric temperature changes, surface pressure changes, and strengthening or weakening of winter cyclones show correlations with the measured or inferred changes in the ionosphere-earth current density J_z in the global electric circuit. These responses are consistent in onset time, duration and sign of the response with the J_z changes associated with both solar activity and internal atmospheric forcing. The responses are consistent with the production of electric space charge in conductivity gradients at the boundaries of cloud and aerosol layers by the flow of J_z through them, and consistent with the theory of electrical effects on scavenging of cloud condensation nuclei and ice-forming nuclei by droplets. However, the overall effect for climate of the consequent variations of cloud cover in latitude, altitude and cloud type remain to be worked out.

The large changes in galactic cosmic ray flux on time scales from decades through millennia produce changes in J_z that have the potential to account for records of long-term climate variations that correlate with cosmic ray flux changes. Also, changes in temperature and humidity in the thunderstorm-generating regions of land masses at low latitudes modulate the current density flowing everywhere in the global circuit. This may affect cloud cover everywhere, especially with surface temperature changes on the longer time scales.

Acknowledgements

This work has been supported by a National Science Foundation grant ATM0242827 to the University of Texas at Dallas, and was approved by the Australian Antarctic Science Advisory Committee (AAS 974). Limin Zhou has been supported in part by a fellowship from the Chinese Academy of Sciences.

References

Adlerman, E.J., Williams, E.R. The seasonal variation of the global electric circuit. J. Geophys. Res. 101, 29679–29688, 1996.

Beard, K.V., Ochs III, H.T., Twohy, C.H. Aircraft measurements of high average charges on cloud drops in layer clouds. Geophys. Res. Lett. 31, L14111, 1–4, 2004.

Bering III, E.A., Few, A.A., Benbrook, J.R. The global electric circuit. Phys. Today 51, 24–30, 1998.

Bond, G., Kromer, B., Beer, J., Muscheler, R., Evans, M.N., Showers, W., Hoffman, S., Lotti-Bond, R., Hagdas, I., Bonani, G. Persistent solar influence on North Atlantic climate during the Holocene. Science 294, 2130–2136, 2001.

Burns, G.B., Frank-Kamenetsky, A.V., Troshichev, O.A., Bering, E.A., Reddell, B.D. Inter-annual consistency of bi-monthly differences in diurnal variations of the ground-level, vertical electric field. J. Geophys. Res. 110, D10106, 1–14, 2005.

Burns, G.B., Tinsley, B.A., Klekociuk, A.R., Troshichev, O.A., Frank-Kamenetsky, A.V., Duldig, M.l., Bering, E.A., Clem, J.M. Antarctic polar plateau vertical electric field variations across heliospheric current sheet crossings. J. Atmos. Solar Terr. Phys. 68, 639–654, 2006.

Burns, G.B., Tinsley, B.A., Troshichev, O.A., Frank-Kamenetsky, A.V., Bering, E.A. Interplanetary magnetic field and atmospheric electric circuit influences on ground level pressure at Vostok. J. Geophys. Res. 112, D04103, 1–10, 2007.

Carslaw, K.S., Harrison, R.G., Kirby, J. Cosmic rays, clouds and climate. Science 298, 1732–1737, 2002.

Cotton, W.R., Anthes, R.A. Storm and Cloud Dynamics. Academic Press, San Diego, 1989.

Eddy, J.A. Climate and the changing sun. Climate Change 1, 173–190, 1977.

Foukal, P. Can slow variations in solar luminosity provide missing link between the Sun and climate? EOS Trans. AGU 84 (22), 205–206, 2003.

Foukal, P., North, G., Wigley, T. A stellar view on solar variations and climate. Science 306, 68–69, 2004.

Frahm, R.A., Winningham, J.D., Sharber, J.R., Link, R., Crowley, G., Gaines, E.E., Chenette, D.L., Anderson, B.J., Potemera, T.A. The diffuse aurora: a significant source of ionization in the middle atmosphere. J. Geophys. Res. 102, 28203–28214, 1997.

Griffiths, R.F., Latham, J., Myers, V. The ionic conductivity of electrified clouds. Quart. J. R. Meteorol. Soc. 100, 181–190, 1974.

Haigh, J.D. The impact of solar variability on climate. Science 272, 981–984, 1996.

Harrison, R.G., Carslaw, K.S. Ion-aerosol cloud processes in the lower atmosphere. Rev. Geophys. 41 (3), 1012, 1–26, 2003.

Hays, P.B., Roble, R.G. A quasi-static model of global atmospheric electricity, 1. The lower atmosphere. J. Geophys. Res. 84, 3291–3305, 1979.

Herman, J.R., Goldberg, R.A. Sun, Weather and Climate. NASA SP-426, Washington, DC, 1978.

Holzworth, R.H., Mozer, F.S. Direct evidence of solar flare modification of stratospheric electric fields. J. Geophys. Res. 84, 363–367, 1979.

Holzworth, R.H., Norville, K.W., Williamson, P.R. Solar flare perturbations in stratospheric current systems. Geophys. Res. Lett. 14, 852–855, 1987.

Hong, Y.T., Jiang, H.B., Liu, T.S., Zhou, L.P., Beer, J., Li, H.D., Leng, X.T., Hong, B., Qin, X.G. Response of climate to solar forcing recorded in a 6000-year $\delta^{18}O$ time-series of Chinese peat cellulose. Holocene 10 (1), 1–7, 2000.

Hoppel, W.A., Frick, G.F. Ion aerosol attachment coefficients and the steady-state charge distribution on aerosols in a bipolar environment. Aerosol Sci. Technol. 5, 1–21, 1986.

Hoyt, D.V., Schatten, K.H. The Role of the Sun in Climate Change. Oxford University Press, New York, 1997.

Hu, H., Holzworth, R.H. Observations and parameterization of the stratospheric electrical conductivity. J. Geophys. Res. 101 (D23), 29535–29552, 1996.

Israël, H. Atmospheric Electricity, vol. II, Israel program for scientific translations, Jerusalem (trans. from German), 1973.

Kirkland, M., Tinsley, B.A., Hoeksema, J.T. Are stratospheric aerosols the missing link between tropospheric vorticity and Earth transits of the heliospheric current sheet? J. Geophys. Res. 101, 29689–29699, 1996.

Kniveton, D.R., Tinsley, B.A. Daily changes in cloud cover and Earth transits of the heliospheric current sheet. J. Geophys. Res. 109, D11201, 1–13, 2004.

Larsen, M.F., Kelley, M.C. A study of an observed and forecasted meteorological index and its relation to the interplanetary magnetic field. Geophys. Res. Lett. 4, 337–340, 1977.

Lean, J., Beer, J., Bradley, R. Reconstruction of solar irradiance since 1610: implications for climate change. Geophys. Res. Lett. 22, 3195–3198, 1995.

Lean, J.L., Yang, Y.-M., Sheeley Jr., N.R. The effect of increasing solar activity on the Sun's total open and magnetic flux during multiple cycles, implications for solar forcing of climate. Geophys. Res. Lett. 29 (24), 2224, 1–4, 2002.

Li, X., Temerin, M., Baker, D.N., Reeves, G.D., Larsen, D. Quantitative prediction of radiation belt electrons at geostationary orbit based on solar wind measurements. Geophys. Res. Lett. 28, 1887–1890, 2001a.

Li, X., Baker, D.N., Kanekal, S.G., Looper, M., Temerin, M. Long term measurements of radiation belts by SAMPEX and their variations. Geophys. Res. Lett. 28, 3827–3830, 2001b.

Luterbacher, J., Rickli, R., Xoplaki, E., Tinguely, C., Beck, C., Pfister, C., Wanner, H. The late Maunder minimum (1675–1715) – a key period for studying decadal scale climate change in Europe. Clim. Change 49, 441–462, 2001.

Macdonald, N.J., Roberts, W.O. Further evidence of a solar corpuscular influence on large scale circulation at 300 mb. J. Geophys. Res. 65, 529–534, 1960.

Mallett, I., Cammas, J.-P., Mascart, P., Bechtold, P. Effects of cloud diabatic heating on the early development of the FASTEX IOP17 cyclone. Q. J. R. Meteorol. Soc. 125, 3439–3467, 1999.

Mansurov, S.M., Mansurova, L.G., Mansurov, G.S., Mikhenvich, V.V., Visotsky, A.M. North-south asymmetry of geomagnetic and tropospheric events. J. Atmos. Terr. Phys. 36, 1957–1962, 1974.

Märcz, F. Short term changes in atmospheric electricity associated with Forbush decreases. J. Atmos. Solar Terr. Phys. 59, 975–982, 1997.

Markson, R. Solar modulation of fair weather and thunderstorm electrification and a proposed program to test an atmospheric electrical sun–weather mechanism, in: McCormac, B.M. (Ed.), Weather and Climate Responses to Solar Variations. Colo. Ass. Univ. Press, Boulder, CO, pp. 323–343, 1983.

McCracken, K.G., Beer, J., McDonald, F.B. Variations of cosmic radiation 1890–1986, and the solar and terrestrial implications. Adv. Space Res. 34, 397–406, 2004.

Meyerott, R.E., Regan, J.B., Evans, J.E. On the correlation between ionospheric potential and the intensity of cosmic rays, in: McCormac, B.M. (Ed.), Weather and Climate Responses to Solar Variations. Colo. Ass. Univ. Press, Boulder, CO, pp. 449–460, 1983.

Misumi, Y. The tropospheric response to the passage of solar sector boundaries. J. Meteorol. Soc. Jpn. 61, 686–694, 1983.

Mühleisen, R., Fischer, H.J., Hoffman, H. Horizontal electric fields in the ionosphere derived from air-electric measurements. Zeit. Geophys. 37, 1055–1059, 1971.

Muscheler, R., Beer, J., Kubik, P.W. Long-term solar variability and climate change based on radionuclide data from ice cores, in: Pap, J., Fox, P. (Eds.), Solar Variability and its Effects on Climate, Geophysical Monograph, vol. 141. AGU Press, Washington, DC, pp. 221–235, 2004.

Neff, U., Burns, S.J., Mangini, A., Mudelsee, M., Fleitmann, D., Matter, A. Strong coherence between solar variability and the monsoon in Oman between 9 and 6 kyr ago. Nature 411, 290–293, doi:10.1038/35077048, 2001.

Olson, D.E. Interpretation of the solar influence on the atmospheric electrical parameters, in: McCormac, B.M. (Ed.), Weather and Climate Responses to Solar Variations. Colo. Ass. Univ. Press, Boulder, CO, pp. 483–488, 1983.

Olson, R.H., Roberts, W.O., Zerefos, C.S. Short-term relationships between solar flares, geomagnetic storms, and tropospheric vorticity patterns. Nature 257, 113–115, 1975.

Page, C.G. The interplanetary magnetic field and sea level pressure, in: Avery, S.K., Tinsley, B.A. (Eds.), Workshop on Mechanisms for Tropospheric Effects of Solar Variability and the Quasi-Bienniel Oscillation. University of Colorado, Boulder, pp. 227–234, 1989.

Pallé, E. Possible satellite perspective effects on the reported correlations between solar activity and clouds. Geophys. Res. Lett. 32, L03802, 1–4, 2005.

Pallé, E., Butler, C.J., O'Brien, K. The possible connection between ionization in the atmosphere by cosmic rays and low level clouds. J. Atmos. Solar Terr. Phys. 66, 1779–1790, 2004.

Park, C.G. Downward mapping of high altitude ionospheric electric fields to the ground. J. Geophys. Res. 81 (1), 168–174, 1976.

Pudovkin, M.I., Veretenenko, S.V. Cloudiness decreases associated with Forbush-decreases of galactic cosmic rays. J. Atmos. Solar Terr. Phys. 57, 1349–1355, 1995.

Ram, M., Stolz, M. Possible solar influences on the dust profile of the GISP2 ice core from central Greenland. Geophys. Res. Lett. 26, 1043–1046, 1999.

Reiter, R.R. Phenomena in Atmospheric and Environmental Electricity. Elsevier, Amsterdam, 1992.

Roldugin, V.C., Tinsley, B.A. Atmospheric transmission changes associated with solar wind-induced ionization variations. J. Atmos. Solar Terr. Phys. 66, 1143–1149, 2004.

Ruddiman, W.F. Earth's Climate Past and Future. W.H. Freeman, NY, 2001.

Sapkota, B.K., Varshneya, N.C. On the global atmospheric electric circuit. J. Atmos. Terr. Phys. 52, 1–20, 1990.

Schuurmans, C.J.E., Oort, A.H. A statistical study of pressure changes in the troposphere and lower stratosphere after strong solar flares. Pure Appl. Geophys. 75, 233–246, 1969.

Shaviv, N.J. Cosmic ray diffusion from the galactic spiral arms, iron meteorites, and a possible climate connection. Phys. Rev. Lett 89, 051102, 1–4, 2002.

Shindell, D., Rind, D., Balachandran, N., Lean, J., Lonergan, P. Solar cycle variability, ozone, and climate. Science 284, 305–308, 1999.

Stott, P.A., Jones, G.S., Mitchell, J.F.B. Do models underestimate the solar contribution to recent climate change? J. Climate 16, 4079–4093, 2003.

Stuiver, M., Grootes, P.M., Braziunas, T. The GISP2 $\Delta^{18}O$ climate record of the past 16,000 years and the role of the sun, ocean and volcanoes. Quart. Res. 44 (3), 341–354, 1995.

Svensmark, H., Friis-Christensen, E. Variation of cosmic ray flux and global cloud coverage: a missing link in sun–climate relationships. J. Atmos. Solar Terr. Phys. 59, 1225–1232, 1997.

Tinsley, B.A. Correlations of atmospheric dynamics with solar wind-induced changes of air-earth current density into cloud tops. J. Geophys. Res. 101 (D23), 29701–29714, 1996.

Tinsley, B.A. Scavenging of condensation nuclei in clouds: dependence of sign of electroscavenging effect on droplet and CCN sizes, in: Proceedings, Int. Conf. on Clouds and Precipitation, p. 248, IAMAS, Bologna, 18–23 July, 2004.

Tinsley, B.A., Deen, G.W. Apparent tropospheric response to MeV–GeV particle flux variations, a connection via electrofreezing of supercooled water in high level clouds? J. Geophys. Res. 96, 2283–2296, 1991.

Tinsley, B.A., Heelis, R.A. Correlations of atmospheric dynamics with solar activity; evidence for a connection via the solar wind, atmospheric electricity and cloud microphysics. J. Geophys. Res. 98 (D6), 10375–10384, 1993.

Tinsley, B.A., Yu, F. Atmospheric ionization and clouds as links between solar activity and climate, in: Pap, J., Fox, P. (Eds.), Solar Variability and its Effects on Climate, Geophysical Monograph, vol. 141. AGU Press, Washington, DC, pp. 321–339, 2004.

Tinsley, B.A., Zhou, L. Initial results of a global circuit model with stratospheric and tropospheric aerosols. J. Geophys. Res. 111, D16205, 1–23, 2006.

Tinsley, B.A., Hoeksema, J.T., Baker, D.N. Stratospheric volcanic aerosols and changes in air-earth current density at solar wind magnetic sector boundaries as conditions for the Wilcox tropospheric vorticity effect. J. Geophys. Res. 99, 16805–16813, 1994.

Tinsley, B.A., Liu, W., Rohrbaugh, R.P., Kirkland, M. South Pole electric field responses to overhead ionospheric convection. J. Geophys. Res. 103 (D20), 26137–26146, 1998.

Tinsley, B.A., Rohrbaugh, R.P., Hei, M. Electroscavenging in clouds with broad droplet size distributions and weak electrification. Atmos. Res. 59-60, 115–136, 2001.

Tinsley, B.A., Zhou, L., Plemmons, A. Changes in scavenging of particles by droplets due to weak electrification in clouds. Atmos. Res. 79, 266–295, 2006.

Todd, M.C., Kniveton, D.R. Changes in cloud cover associated with Forbush decreases of galactic cosmic rays. J. Geophys. Res. 106, 32031–32042, 2001.

Twomey, S. The influence of pollution on the shortwave albedo of clouds. J. Atmos. Sci. 34, 1149–1152, 1977.

Usoskin, I.G., Marsh, N., Kovaltsov, G.A., Mursula, K., Gladysheva, O.G. Latitudinal dependence of low cloud amount on cosmic ray induced ionization. Geophys. Res. Lett. 31, L16109, 1–4, 2004.

van Delden, A. On the deepening and filling of balanced cyclones by diabatic heating. Meteorol. Atmos. Phys. 41, 127–145, 1989.

Veretenenko, S., Thejll, P. Effects of energetic solar protons events on the cyclone development in the North Atlantic. J. Atmos. Solar Terr. Phys. 66, 393–405, 2004.

Veretenenko, S., Thejll, P. Cyclone regeneration in the North Atlantic intensified by energetic solar proton events. Adv. Space Res. 35, 470–475, 2005.

Voiculescu, M., Usoskin, I.G., Mursula, K. Different responses of clouds to solar input. Geophys. Res. Lett. 33, L21802, 1–4, 2006.

Wang, Y., Cheng, H., Edwards, R.L., He, Y., Kong, X., An, Z., Wu, J., Kelly, M.J., Dykoski, C.A., Li, X. The Holocene Asian monsoon: links to solar changes and North Atlantic climate. Science 308, 854–857, 2005a.

Wang, Y.-M., Lean, J.L., Sheeley Jr., N.R. Modeling the sun's magnetic field and irradiance since 1713. ApJ 625, 522–538, 2005b.

Wilcox, J.M., Scherrer, P.H., Svalgaard, L., Roberts, W.O., Olson, R.H. Solar magnetic structure: relation to circulation of the Earth's atmosphere. Science 180, 185–186, 1973.

Williams, E.R. Lightning and climate: a review. Atmos. Res. 76, 272–287, 2005.

Yu, F., Turco, R.P. From molecular clusters to nanoparticles: the role of ambient ionization in tropospheric aerosol formation. J. Geophys. Res. 106, 4797–4814, 2001.

Zhao, X., Hundhausen, A.J. Spatial structure of the solar wind in 1976. J. Geophys. Res. 88, 451–454, 1983.

Zhou, L., Tinsley, B.A. The production of space charge in layer clouds, J. Geophys. Res, in press.